Modeling of Multi Phase Flow in Porous Media: Operator Splitting, Front Tracking, Interfacial Area and Network Models

PhD Thesis in Applied Mathematics

Hans Fredrik Nordhaug

Department of Mathematics
University of Bergen

October 2001

Preface

An introductory note together with a collection of papers constitute my thesis presented in partial fulfillment of the requirements for the degree of Doctor Scientarum in applied mathematics at the Department of Mathematics, University of Bergen. The study started formally September 1998 and lasted over three years.

In this work several new numerical methods and a new mathematical model related to multi phase flow in oil reservoirs have been developed, implemented and tested. The numerical difficulties in multi phase flow stem from the highly nonlinear nature of the equations. The solution can develop sharp fronts that travel through the reservoir. We have used front tracking to capture these fronts in our numerical methods. In addition *corrected* operator splitting for systems has been used and developed because of the advection dominated nature of the equations. The new mathematical model was developed to improve short comings of existing models and to include interfacial area as a new independent variable.

This thesis consists of two parts. Part I, the introduction, is a summary of the papers presented in Part II. Some additional results that did not appear in the papers are also included in Part I. Part II consists of the following 5 papers:

Operator splitting methods for systems of convection-diffusion equations: Nonlinear error mechanisms and correction strategies

> This paper presents a modification of corrected operator splitting for scalar equations to systems. The idea is to construct a residual flux after the advection step and use this flux in the diffusion step.

A local streamline Eulerian-Lagrangian method for two-phase flow

> Two dimensional two-phase flow is solved by operator splitting. The advection part is solved by front tracking along streamlines, and the diffusion part by a standard finite difference scheme.

A streamline front tracking method for two- and three-phase flow including capillary forces

> Two dimensional multiphase flow is solved by operator splitting. The advection part is solved by front tracking along streamlines, and the diffusion part by a standard finite difference scheme. The method is compared to a fast marching method and a modified method of characteristics.

Two phase flow including interfacial area as a variable

> In this paper a new model for two phase flow in porous media is presented. Starting out from a model that covers all the physics we make simplifying assumptions. The resulting model includes interfacial area as one of the dependent variables.

A pore network model for calculation of interfacial velocities

> A simple dynamic network model (presented by Blunt & King) is used to calculate saturations, interfacial area, pressures and velocities. Since the results are obtained at a micro scale averaging is done to obtain macroscale variables like pressure and saturations. The averaged results are used to test the equations proposed in the paper above.

In more detail Part I consists of 5 chapters. Chapter 1 gives a short general introduction to multi phase flow in porous media. Some of the main physical and numerical problems investigated in this work are presented here. The subsequent three chapters in Part I give summaries of the papers: Chapter 2 gives a brief description of corrected operator splitting for systems. In Chapter 3 front tracking along stream lines is explained. Finally in Chapter 4 inclusions of interfacial area in two phase flow models and dynamic network models are discussed. Chapter 5 gives a general summary of conclusions and remarks.

The numerical models used in this thesis are written in either C, C++ or Fortran 77 and used under all or some of the following environments: Linux, Unix and Windows. Matlab has been extensively used, but mostly as a visualization tool. The thesis is written in LaTeX and the editor of my choice is Emacs.

Acknowledgments

This work was supported by the Norwegian Research Council (NFR) under grant 116153/431.

At the end of this project there are a lot of people I wish to thank. First of all, I wish to express my sincere gratitude to my supervisor Helge K. Dahle. Without his help this would never have come to an end. I also would like to express my gratitude to my co-supervisors Magne S. Espedal and Kenneth H. Karlsen. They have all contributed with their insights and interesting discussions.

There have been several others involved in this project, but in particular I would like to thank William G. Gray and Michael A. Celia. Without their deep insights some of the main ideas would never have emerged.

The fall 2000 I stayed as a guest researcher at the department of Civil and Environmental Engineering at Princeton University, New Jersey, USA. My advisor there was Michael A. Celia. I am very grateful to him that he made it possible for me to come and that he made it such an interesting stay. I would also like to thank Rudolph Held and Twan Gielen for interesting discussions during this period.

The three years at the department has been a nice time thanks to the colleagues in my group, LIM – Laboratory of Industrial Mathematics, and the students at the sixth floor. No one mentioned, no one forgotten.

And last, but not least, I would like to thank my girlfriend Celia M. Berg.

Hans Fredrik Nordhaug
Bergen, October 2001

Contents

Part I

Introduction

Chapter 1

Multi phase flow in porous media

In reservoir problems we consider some or all of the following phases: Oil, gas, water and solid. The solid phase is normally assumed to be immobile and non-deforming, but in general this does not need to be the case. By multi phase flow we will mean the flow of oil, gas and water. The phases are categorized according to their different physical quantities. A hydrocarbon phase, may consist of different hydrocarbon components, e.g., the oil phase can contain several oil and gas types. In this work the components are neglected and only the phases are considered. A porous medium is any solid phase, e.g. sand stone, that is permeable. The flow in a porous medium takes place through connected pores in the rock. Regions on a larger scale that contain oil or gas are called reservoirs. The typical size of a reservoir is kilometers in each direction while the pore scale size is millimeters or less. Solving the Navier-Stokes equation at the pore scale to obtain the transport on a larger scale is not numerically feasible because of the huge difference in scales. Therefore, some averaging is necessary to go from the pore scale (micro scale) to the reservoir scale (macro scale). In this process the Navier-Stokes equations are replaced by macro scale equations that are solved for macro scale variables. For a thorough introduction to reservoir modeling see [1].

The papers presented herein cover several topics in multi phase flow in porous media, and they address some central problems both on the micro scale as well as on the macro scale. In addition, operator splitting techniques have been developed for convection dominated non-linear transport equations.

1.1 From micro to macro scale

As noted above it is not numerically feasible to solve the equations on the micro scale to obtain macro scale behavior for the fluid phases. Therefore macro scale equations involving macro scale variables are used. Traditional multi-phase

flow models are usually based on direct extensions of one-phase flow equations like Darcy's law and conservation of mass. This leads to the introduction of constitutive relationships like capillary pressure curves and relative permeabilities. Although such models are generally accepted and have been successfully applied to numerous problems, one can easily list several difficulties. Most important, the models are ad hoc and involve hidden assumptions.

A rigorous approach to modeling of multi-phase flow is given by Gray and Hassanizadeh, e.g. [2]. This approach starts from first principles and is aiming at a more complete description of multi-phase flow phenomena. By using localization theorems the authors transform conservation equations for micro scale variables to conservation equations for macro scale variables. These theorems essentially transform averages of derivatives to derivatives of averages. In Paper D we use this approach to get a new formulation for two phase flow including interfacial area. Some of the proposed equations in this work are tested using a dynamical network model in Paper E.

Since geological data currently is available at a much finer scale than any practical computational grid, some kind of upscaling is necessary to get reasonable averaged physical parameters. This kind of parameter upscaling is not the subject of this work, and we refer to Dagan [3] for a thorough description of different scales in porous media flow and averaging techniques. However, we note that as the computers become faster and the methodologies improve, the computational scale may get closer to the geological scale. Some of the methods described in this work are aiming in that direction.

1.2 Non-linear equations and systems

Mathematical models for fluid flow often involve systems of convection-diffusion equations. This is the case for multi phase flow in porous media. These models are normally convection dominated with sharp fronts building up because of the non-linearities in the flow functions. Because of these fronts, difficulties will be experienced when standard numerical approximations are used. Thus, many different methods have been proposed to overcome the difficulties, see [4].

Mathematical models for three phase flow models often consist of a set of pressure–velocity equations and a pair of strongly coupled equations for phase saturations. The set of saturation equations is normally called a 2×2 system. The coupling of these strongly non-linear equations makes them hard to solve. In Paper C (and A), a solution procedure for a simplified 2×2 system is presented. We assume that one of the phases is independent of the other. This will normally be the gas and is due to the fact that the viscosity of the gas phase is usually at least an order less than the viscosities of the liquid phase(s). We call such a system

a triangular system because the Jacobi matrix for the flow functions is upper (or lower) triangular.

An important design principle for many numerical methods for convection-diffusion equations is *operator splitting* (OS). That is, one splits the time evolution into partial steps to separate the effects of convection and diffusion. It has been shown that the temporal splitting error can be significant when there is a shock present in the solution. This is well understood for scalar convection-diffusion equation. Paper A describes the error mechanisms and a correction strategy for systems.

In Paper A, B and C we concentrate on finding accurate and efficient solvers for the advection step in the OS method. To achieve high efficiency, i.e, long time steps, we have chosen to use the front tracking algorithm. The algorithm itself is super fast and has no numerical diffusion. However, front tracking relies on accurate Riemann solvers, and for systems in general they are hard to construct. For a certain class of triangular 2×2 systems the Riemann solver is not too complicated to construct, and in Paper C (and A) we have solved such systems by using front tracking.

Chapter 2

Corrected operator splitting for systems

This chapter describes the methods and ideas from Paper A, "*Operator splitting methods for systems of convection-diffusion equations: Nonlinear error mechanisms and correction strategies* ".

Mathematical models for fluid flow often involve systems of convection-diffusion equations as a main ingredient. As mentioned in Section 1.2, operator splitting (OS) is an important tool for developing numerical methods for such systems. In particular, OS methods are often used to solve convection-diffusion problems that are of convection dominated nature, see [5] and the references therein.

2.1 Introduction

The motivation for operator splitting methods is that it is easy to combine efficient methods for solving the convection step with efficient methods for solving the diffusive step. Especially for convection dominated systems, it is a major advantage to be able to use an accurate and efficient hyperbolic solver developed for tracking discontinuous solutions. By combining this with efficient methods for the diffusive step, we get a powerful and efficient numerical method which is well suited for solving parabolic problems with sharp gradients.

The obvious disadvantage of operator splitting methods is the temporal splitting errors. The temporal splitting error in OS methods can be significant in regions containing viscous shocks [6, 7, 8]. Thus, to resolve viscous shock profiles correctly, one must resort to very small splitting steps. This imposes a time step restriction that is not present in the underlying numerical methods for the convective and the diffusive step. To reduce the influence of temporal splitting errors in OS methods, and to allow for the use of large splitting steps, the *corrected oper-*

ator splitting (COS) method was introduced by Espedal and Ewing [9]. A recent mathematical description of this method was given by Karlsen and Risebro [10].

The main idea behind the scalar COS method is to take into account the unphysical entropy loss (due to Oleinik's convexification [11]) produced by the hyperbolic solver in the convective step. The COS approach uses the wave structure from the convective step to identify where the (nonlinear) splitting errors occur.

The purpose of the paper described here is to derive a thorough understanding of the nonlinear mechanisms behind the viscous splitting error typically appearing in operator splitting methods for systems of convection-diffusion equations. This mechanism is well understood in the scalar case.

2.2 Operator splitting

To describe our ideas in more detail, we consider the one dimensional Cauchy problem for $\ell \times \ell$ ($\ell \geq 1$) systems of convection-diffusion equations

$$\partial_t U + \partial_x F(U) = D\,\partial_x^2 U, \qquad U(x,0) = U_0(x) \tag{2.1}$$

where $x \in \mathbb{R}$ and $t > 0$. Here $U = (u_1, \ldots, u_\ell)^{\mathrm{T}}$ is the unknown state vector, $F(U) = (f_1(U), \ldots, f_\ell(U))^{\mathrm{T}}$ is a vector of flux functions for each variable, and $D = \mathrm{diag}(\varepsilon_1, \ldots, \varepsilon_\ell) > 0$ is a constant diagonal matrix. Let $\mathcal{S}_t$ denote the solution operator which takes the initial data $V_0(x)$ to a weak solution at time t of the purely hyperbolic problem

$$\partial_t V + \partial_x F(V) = 0, \qquad V(x,t) = V_0(x). \tag{2.2}$$

We write $V(x,t) = \mathcal{S}_t V_0(x)$ for this weak solution. Next, let $\mathcal{H}_t$ denote the operator which takes the initial data $W_0(x)$ to a weak solution at time t of the purely parabolic problem

$$\partial_t W = D\partial_x^2 W, \qquad W(x,t) = W_0(x). \tag{2.3}$$

We write $W(x,t) = \mathcal{H}_t W_0(x)$ for this solution.

In what follows, we consider a fixed final computing time $T > 0$. For simplicity we also choose a fixed splitting step $\Delta t > 0$ and an integer N_t such that $N_t \Delta t = T$. Then we define the semi-discrete OS algorithm by

$$U_{\Delta t}(\cdot, n\Delta t) := \left[\mathcal{H}_{\Delta t} \circ \mathcal{S}_{\Delta t}\right]^n U_0(\cdot), \qquad n = 0, \ldots, N_t. \tag{2.4}$$

In applications, the exact solution operators $\mathcal{S}_t$ and $\mathcal{H}_t$ in (2.4) are replaced by numerical methods. We will use front tracking as defined by Risebro [12, 13, 14] as an approximate solution operator for the hyperbolic part. For the parabolic part, we here use a simple explicit central difference method.

2.3 Nonlinear error mechanisms

In the introduction we stated that OS approximations can be too diffusive near viscous shocks when the splitting step Δt is large. To explain this in more detail let us first study the *scalar* case:

The entropy condition introduces a local linearization of $f(\cdot)$ once a shock is formed in the convection step. This linearization represents the entropy loss associated with the formation of a shock in the hyperbolic solution. Thus, the evolution of the *hyperbolic* solution is governed locally by some convex/concave envelope f_c of f between the left and right shock values, see Figure 2.1. A similar linearization can be introduced locally for the *parabolic* problem. That is, the flux function f can be decomposed into a convective part f_c and a self-sharpening part $f - f_c$ that tends to counteract the diffusive forces. Loosely speaking, we say that f_c governs the local translation and $f - f_c$ the shape (or structure) of the viscous front. In the OS algorithm, the local residual flux $f - f_c$ is disregarded in the hyperbolic step and the corresponding self-sharpening effects are therefore not taken into account in the splitting, resulting in a splitting error. Figure 2.1 gives an illustration of f, f_c, and the residual flux $f_{\text{res}} := f - f_c$ in the scalar case.

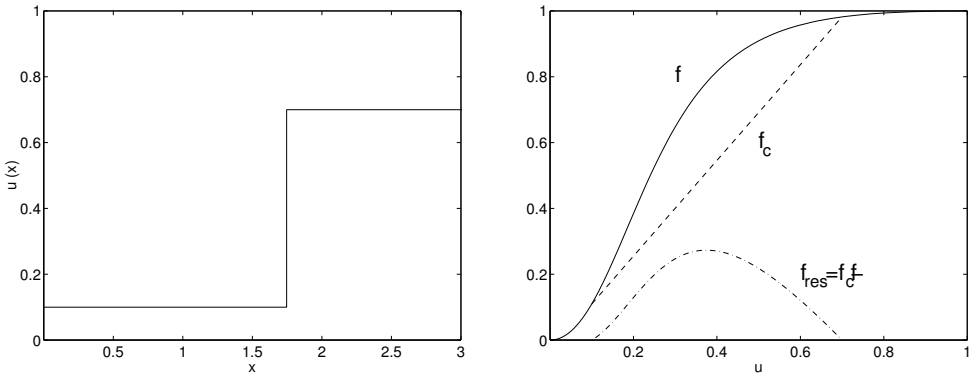

Figure 2.1: (Left) A single shock solution from a convection step. (Right) The corresponding residual flux function; flux function f (solid), convex envelope f_c, i.e., local linearization (dash), and residual flux f_{res} (dash-dot).

For a general system, the error mechanism is quite similar. To study it, we consider the propagation of a single viscous shock. Assume that the splitting step is sufficiently large so that a shock has developed in the hyperbolic substep (2.2), i.e., the solution $V(\cdot, t = \overline{t})$ consists of a single discontinuity at $x = \overline{x}$ with left and right shock values $V^l = (v_1^l, \ldots, v_1^l)^{\mathrm{T}}$ and $V^r = (v_1^r, \ldots, v_1^r)^{\mathrm{T}}$. Then the behavior (forward and backward in time) of $V(x, t)$ locally around $(\overline{x}, \overline{t})$ is governed by the

linearized hyperbolic problem

$$\partial_t V + \partial_x(\bar{\sigma} V) = 0, \qquad V(x,\bar{t}) = \begin{cases} V^l, & \text{for } x < \bar{x}, \\ V^r, & \text{for } x > \bar{x}, \end{cases} \tag{2.5}$$

where $\bar{\sigma}$ is the Rankine–Hugoniot shock speed satisfying

$$F(V^l) - F(V^r) = \bar{\sigma}(V^l - V^r).$$

We *claim* that a large part of the splitting error that occurs locally around $(\bar{x},\bar{t})$ in the standard OS algorithm can be understood in terms of the difference between the nonlinear system (2.1) and the linearized system (2.5) with right-hand side $D\partial_x^2 V$. In other words, in terms of the difference $\partial_x(F(U) - \bar{\sigma}U)$. In (2.1), the diffusion caused by the second order operator is perfectly balanced by the self-sharpening effects due to the nonlinearity in the convective operator. In the OS strategy, this self-sharpening disappears once a shock develops because $F(U)$ is in effect replaced by $\bar{\sigma}U$ locally. Thus, one step in OS effectively amounts to solving $\partial_t U + \partial_x(\bar{\sigma}U) = D\partial_x^2 U$ and not (2.1).

2.3.1 The COS strategy

To compensate for the loss of self-sharpening effects, the *scalar* COS approach proposes to include the residual flux F_{res} in the diffusion step of the splitting. The COS method therefore replaces the purely parabolic split problem (2.3) by

$$\partial_t W + \partial_x F_{\text{res}}(x, W) = D\partial_x^2 W, \qquad W(x,0) = W_0(x). \tag{2.6}$$

where $F_{\text{res}}(x, W)$ is the residual flux in the point x. Letting $\mathcal{P}_t$ denote the solution operator associated with (2.6), the COS solution may then be defined as

$$U_{\Delta t}(\cdot, n\Delta t) := \left[\mathcal{P}_{\Delta t} \circ \mathcal{S}_{\Delta t}\right]^n U_0(\cdot). \tag{2.7}$$

We have replaced the convection-diffusion equation (2.1) by a hyperbolic equation (2.2) and another convection-diffusion equation (2.6), where the flux term in (2.6) is seemingly more complicated than the one in (2.1). However, we see that while F contains convective *and* self-sharpening effects, F_{res} only contributes to self-sharpening effects. Thus, viscous shock fronts are moved to the correct location in the convective step and given a correct shape in the diffusive step.

When applied to systems of parabolic equations, the correction algorithm needs to be reformulated, since one cannot simply write down the solution of the hyperbolic step in terms of convex/concave envelopes. Instead, we identify the following term

$$\partial_x F_{\text{res}}(U) = \partial_x\big(F(U) - \bar{\sigma}U\big), \tag{2.8}$$

for each discontinuity in the solution from the hyperbolic step. Then, the parabolic subproblem (2.3) is modified locally by adding $F_{\text{res}}(U)$, which gives the new split problem (2.6). By integrating (2.8) with respect to x, we get the *residual flux*

$$F_{\text{res}}(U) = \big(F(U) - F(V^l)\big) - \bar{\sigma}\big(U - V^l\big), \tag{2.9}$$

where we have chosen the constant of integration such that

$$F_{\text{res}}(V^l) = F_{\text{res}}(V^r) \equiv 0.$$

2.4 A COS method

The operator splitting methods introduced above result in two different subproblems that each must be solved numerically. The convection part is solved by a front tracking method, and the diffusion part is solved by an explicit central finite difference scheme.

2.4.1 Convection solver

In this section we describe the front tracking method [12, 13, 14] for solving systems of conservation laws (2.2)

$$\partial_t V + \partial_x F(V) = 0, \quad V(x,0) = V_0(x).$$

Front tracking is an algorithm for computing a piecewise constant approximation to $V(x,t)$. The advantage of using a front tracking method is that it directly identifies the correct physical envelope, given that the Riemann solver is correct. We will not discuss Riemann solvers further here, but just note that finding good approximative Riemann solvers for systems is in general a difficult problem. Descriptions of the Riemann solvers used in the applications are given in Section 3 in Paper A.

First, V_0 is approximated by a step function so that a Riemann problem can be associated with each jump in the approximate initial data. The solution of each Riemann problem is approximated by step functions. In the front tracking approximation, rarefaction waves are approximated by step functions sampled along the wave curves (according to a pre-set, user-defined parameter δ), while the rest of the Riemann solution is left intact. By doing this each Riemann problem produces a sequence of jump discontinuities (fronts) that travel with a finite wave speed. The Riemann solution is represented by a list of fronts, sorted according to increasing wave speeds. A global solution (in x) is formed by connecting the local Riemann solutions. The solution consists of constant states separated by space-time rays, i.e., a list of fronts sorted from left to right. There will be a first time

at which two or more space-time rays intersect, i.e., two or more fronts collide. This collision defines a new Riemann problem which is solved and inserted into the list. The algorithm proceeds in this manner from collision to collision. The numerical method is *unconditionally* stable and very fast.

2.4.2 Diffusion solver

The parabolic step is a Cauchy problem of the form

$$\partial_t W + \partial_x G(W) = D\partial_x^2 W, \quad W(x,0) = W_0(x). \tag{2.10}$$

In applications G is the residual flux term, see (2.8), and D is still the diagonal matrix $\mathrm{diag}(\varepsilon_1,\ldots,\varepsilon_\varrho) > 0$. To solve this system, one can for instance use the explicit, central finite difference method

$$\frac{W_j^{n+1} - W_j^n}{\tau} - \frac{G(W_{j+1}^n) - G(W_{j-1}^n)}{2\Delta x} = D\frac{W_{j+1}^n - 2W_j^n + W_{j-1}^n}{(\Delta x)^2}. \tag{2.11}$$

This scheme is stable provided the discretization parameters τ and Δx satisfy the following conditions

$$\tau \le 0.5\Delta x^2 / \max \varepsilon_i, \qquad \Delta x \max|\lambda_G| \le 2\max \varepsilon_i,$$

where λ_G denotes the eigenvalues of G', the derivative of G. See Strikwerda [15] for an introduction to finite difference schemes and this one in particular. For the Cauchy problem (2.10), which has linear diffusion, convergence and error estimates for this scheme is shown in [16]. The stability conditions above may put severe restrictions on the discretization parameters, especially on Δx for small values of ε. However, both these conditions can be weakened or removed by using a more sophisticated scheme. The use of implicit schemes is discussed in the next section. To keep the technical details at a minimal level, we chose the simple explicit scheme.

2.4.3 Construction of the residual flux

Given a piecewise constant front tracking solution, $U^{n+1/2}$, of the hyperbolic equation (3.4), we can now construct the residual flux $F_{\mathrm{res}}(x,\cdot)$ appearing in (2.6). We assume that the discontinuities of $U^{n+1/2}(x)$ are located at the points $\{x_i\}$. Let $U_i = (u_1^i,\ldots,u_\varrho^i)^{\mathrm{T}}$ and $U_{i+1} = (u_1^{i+1},\ldots,u_\varrho^{i+1})^{\mathrm{T}}$ denote the values of $U^{n+1/2}(x)$ in the intervals $[x_{i-1},x_i)$ and $[x_i,x_{i+1})$, respectively. Locally, around the ith discontinuity emerging from (x_i,t_0) the nonlinear problem (2.2) is governed by the

linearized problem

$$\partial_t V + \partial_x(\sigma_i V) = 0, \qquad V(x_i, t_0) = \begin{cases} U_i, & \text{for } x < x_i, \\ U_{i+1}, & \text{for } x > x_i, \end{cases}$$

where σ_i is the Rankine–Hugoniot shock speed satisfying $F(U_i) - F(U_{i+1}) = \sigma_i(U_i - U_{i+1})$. Motivated by the discussion in Section 2.3, we define the residual flux F^i_{res} associated with the ith discontinuity, as

$$F^i_{\text{res}}(U) = \begin{cases} \big(F(U) - F(U_i)\big) - \sigma_i\big(U - U_i\big), & U \in (u_1^i, u_1^{i+1}) \times \cdots \times (u_\varrho^i, u_\varrho^{i+1}), \\ 0, & \text{otherwise.} \end{cases}$$

Note that $F^i_{\text{res}}(U_i) = F^i_{\text{res}}(U_{i+1}) \equiv 0$.

Although a residual flux term can be identified for every discontinuity in the front tracking solution, they should not be included for discontinuities which approximate rarefaction waves or for weak shocks. Therefore, in practice, we only include residual terms for shock waves with strength exceeding a user-defined threshold parameter γ. The process of identifying relevant residuals can be made more rigorous, and simplified, by tagging fronts in the front tracker according to wave type (shock/rarefaction/contact).

Having defined the residual fluxes in state space $(u_1, \ldots, u_\varrho)$, we need to specify where to apply them in physical space (i.e., intervals in x). For *explicit* discretizations we apply the following strategy: Observe that in each spatial interval where the solution is monotone in all its components (henceforth called *monotonicity interval*), all residual fluxes are defined on disjoint sets in state space. Therefore, the residual flux is set to zero outside (a subset of) the associated monotonicity interval, i.e.,

$$F_{\text{res}}(x, U) = \sum_i F^i_{\text{res}}(U)\chi_{D_i}(x),$$

where $\chi_I(x)$ denotes the indicator function of the interval $I \subset \mathbb{R}$ and D_i is the (subset of) the monotonicity interval. For implicit discretizations we use a much simpler approach where the user prescribes the length of the intervals where the correction is applied. Unfortunately, specifying a reasonable length for the correction intervals must be based on experience. For further details concerning the construction of the residual flux we refer to Paper A.

2.5 Concluding remarks

In Paper A results for two particular 2×2 systemsdescribing flow in porous media were presented. Simulations for a two-phase multicomponent model, a polymer

system, and for a triangular three-phase flow model were reported. In addition, the polymer system is solved in 2D using dimensional splitting.

We demonstrate numerically that operator splitting (OS) methods for systems of convection-diffusion equations in one space dimension, have a tendency to be too diffusive near viscous shock waves. The idea behind the scalar COS method is to use the wave structure from the convection step to identify where the nonlinear splitting error (or entropy loss) occurs. The potential error is then compensated for in the diffusion step (or in a separate correction step).

Similar to the scalar case, the splitting error is closely related to the local linearizations introduced implicitly in the convection steps due to the use of an entropy condition. A COS method for systems was proposed. The numerical examples demonstrate that the COS method is significantly more accurate than the corresponding OS method when the splitting step is large and the solution consists of (moving) viscous shock waves.

Chapter 3

Solving multi dimensional multi-phase flow by front tracking along streamlines

This chapter describes the results and ideas form Paper B, *"A local streamline Eulerian-Lagrangian method for two-phase flow "*, and Paper C, *"A streamline front tracking method for two- and three-phase flow including capillary forces "*.

Increased demands for assessment of uncertainties and history matching require fast and accurate flow simulations on multiple plausible geological models on a routinely basis. Conventional reservoir simulators fail to fulfill this need, and there seems to be a trend within the petroleum industry to simulate reduced sets of equations. Typically streamline and/or front tracking methods are used to solve the hyperbolic Buckley-Leverett equation for two-phase flow, see [17, 18, 19].

In the work described here we consider models of multi-phase flow which do include capillary forces. We also allow for three phases. In particular we shall investigate a streamline front tracking method. To account for capillary effects we use operator splitting [5]. We compare the streamline front tracking method (SFTM) with a fast marching method (FFM) and a modified method of characteristics (MMOC).

3.1 Governing equations

The basic equations describing three-phase immiscible flow in a porous medium, say water (w), gas (g) and oil (o), are mass balance equations and Darcy's law. Assuming that the flow is incompressible, and that gravity can be neglected, the equations can be written in a global pressure/total velocity formulation, see [20,

21], as follows:

$$\nabla \cdot \mathbf{v} = q(\mathbf{x}, t), \tag{3.1}$$

$$\mathbf{v} = -\lambda_T(\mathbf{x}, S_\alpha)\mathbf{K}(\mathbf{x}) \cdot \nabla p, \tag{3.2}$$

$$\phi \frac{\partial S_\alpha}{\partial t} + \nabla \cdot [F_\alpha \mathbf{v} - \epsilon_\alpha \nabla \cdot D_\alpha(\mathbf{x}, S_\alpha) \nabla S_\alpha] = q_\alpha(\mathbf{x}, t). \tag{3.3}$$

Here ϕ and $\mathbf{K}(\mathbf{x})$ are the porosity and absolute permeability of the porous medium; S_α, $\mathbf{v}_\alpha$, $k_{r\alpha}$, μ_α and q/q_α are, respectively, the reduced phase saturation, Darcy velocity, relative permeability, viscosity of phase α and sink/source terms. A global pressure p is derived from the phase pressures and the capillary pressures, see [21]. We refer to Paper B and C for more details on this standard formulation.

3.2 Solution strategy

To decouple the Pressure/Velocity equations (3.1), (3.2), from the saturation equations (3.3), we use sequential time stepping. Thus, for a given saturation-field, say at time t^n, we calculate a new velocity field. The saturation field is then advanced to a new time-step t^{n+1} by solving (3.3), using the most recent velocity field. This is continued sequentially up to a predetermined time $t = T$.

To solve the parabolic saturation Equation (3.3) with a given velocity field, we again use operator splitting as described in Section 2.2 on page 8. In previous works a Modified-Method-of-Characteristics (MMOC) has been used to solve the two-phase flow problem based on the ideas outlined above, see [22]. This method works excellently when the wave structure of the solution is known a priori. We present two alternative methods to the MMOC method, which both preserve the shape of self-sharpening fronts and are more flexible than the MMOC method in the sense that no a priori knowledge of the wave structure is required.

3.2.1 A streamline front tracking method

For simplicity we assume that the computational domain is discretized by a regular Cartesian grid such that the velocity $\mathbf{v} = \mathbf{v}(\mathbf{x}) \in RT_0$ is given, where RT_0 is the lowest order Raviart-Thomas space. Furthermore, we assume that all variables are known at cell centers at time-level t^n.

To obtain saturation values S^{n+1} at time-level t^{n+1}, we split Equation (3.3) into a hyperbolic equation

$$S_t + \mathbf{v} \cdot \nabla F(S) = 0, \tag{3.4}$$

and a parabolic heat type equation

$$S_t = \epsilon \nabla \cdot (D \nabla S). \tag{3.5}$$

where S and $F(S)$ are vectors of saturations and fluxes, respectively. The equations are solved in a standard operator splitting fashion, see previous chapter.

Now, consider the solution of Equation (3.4). Observe that on streamlines $\mathbf{r} = \mathbf{r}(\xi)$ such that

$$\frac{d\mathbf{r}}{d\xi} = \mathbf{v}, \tag{3.6}$$

Equation (3.4) becomes one-dimensional

$$S_t + F_\xi(S) = 0. \tag{3.7}$$

We exploit this to obtain new saturation-values at cell centers $\mathbf{x}_I$, in the following way: First, trace streamlines (3.6) analytically for $\mathbf{r}(0) = \mathbf{x}_I$ and $-\xi_{\max} < \xi < \xi_{\max}$. Here $\xi_{\max} = |\lambda_{\max}|(t^{n+1} - t^n)$ with $\lambda_{\max}$ being an estimate of the maximum wave speed of the system, such that the streamline covers the domain of dependence for $(\mathbf{x}_I, t^{n+1})$. The streamline is only traced in the upstream direction if all the wave speeds are positive. The piecewise constant cell values of the saturations are then projected onto these local streamlines, thus defining piecewise constant initial conditions for Equation (3.7). This conveniently arranges for Equation (3.7) to be solved by the front tracking method. (See Section 2.4.1 on page 11 for a description of the method.)

The main advantages of the front tracking method, is that the method is super fast [23], and preserves the frontal structure of the solutions extremely well. On the other hand, since the method heavily depends on solving Riemann problems, it is not easy to extend the method to three-phase flow. In Section 3.3, we will discuss a solution strategy for so-called triangular systems which may be a step towards an applicable solution procedure for three-phase flow problems.

Equation (3.5) may be solved by finite element or finite difference based methods. In this work we have for convenience used a standard explicit central finite difference scheme. Note that a local time step, $\Delta t_{\text{diff}} \leq t^{n+1} - t^n$, is required to satisfy the stability constraint inherent in the explicit finite difference method.

3.3 Triangular systems

A possible extension of the SFTM approach to three-phase flow, is to use an approximate Riemann solver to generate front speeds. However, to our knowledge, the construction of accurate and reliable Riemann solvers for fully coupled three-phase flow is not a trivial task, and we have chosen a different approach here.

Observe that the viscosity of the gas phase is usually at least an order less than the viscosities of the liquid phases. Motivated by this fact, it seems reasonable to assume that the fractional flow function of the gas phase can be approximated by a flux function which only depends on the saturation of the gas phase. Thus, we may consider the following 2×2-triangular hyperbolic system, as an approximation to the hyperbolic part of the fully coupled system (3.3):

$$\frac{\partial S_g}{\partial t} + \frac{\partial}{\partial x} F_g(S_g) = 0, \tag{3.8}$$

$$\frac{\partial S_w}{\partial t} + \frac{\partial}{\partial x} F_w(S_g, S_w) = 0. \tag{3.9}$$

Systems of this type have been investigated in [24, 25, 26], and existence and uniqueness of the solution to the Riemann problem is shown under general conditions.

3.3.1 A Riemann solver for triangular systems

The numerical construction of a solution for a Riemann problem associated with equations (3.8)-(3.9) was developed by Gimse [24]. The idea is to solve the Riemann problem for (3.8) first. The approximate solution to (3.8) consists of a set of constant states, say $S_g^L = S_g^1 < S_g^2 < \ldots < S_g^{N+1} = S_g^R$, separated by jump discontinuities traveling with the Rankine-Hugoniot shock speed:

$$s_i = \frac{F_g(S_g^{i+1}) - F_g(S_g^i)}{S_g^{i+1} - S_g^i}, \quad i = 1, 2, \ldots, N. \tag{3.10}$$

Within each wedge of the solution fan, the fractional flow of the water phase depends only on the water saturation and is given as:

$$F_w^i(S_w) \stackrel{\text{def}}{=} F_w(S_g^i, S_w), \quad i = 1, 2, \ldots, N+1.$$

Thus, we may easily solve for the water saturation within each wedge once we know the left- and right-hand state of the water saturation within the wedge. Obviously, successive left- and right-hand states over the discontinuities in the gas phase must also satisfy the jump condition

$$\frac{F_w^{i+1}(S_w^{i+1}) - F_w^i(S_w^i)}{S_w^{i+1} - S_w^i} = s_i, \quad i = 1, 2, \ldots, N, \tag{3.11}$$

There are infinitely many states S_w^i, which satisfy conditions (3.11), leading to the definition of the so-called H-sets:

$H_{1,in}$ The set of S_w-values in region S_g^L, that can be reached from S_w^L with speed $\sigma \leq s_1$.

$H_{i,in}$ The set of S_w-values in region S_g^i, $i = 2, 3, \ldots N$, that can be reached from $H_{i,out}$ with speed σ such that $s_{i-1} \leq \sigma \leq s_i$.

$H_{i+1,out}$ The set of S_w-values in region S_g^{i+1}, $i = 1, 2, \ldots N+1$, that can be reached from $H_{i,in}$ by a shock with speed s_i.

The solution can now be assembled by connecting the right state, S_w^R, to the left state, S_w^L, by admissible waves given by the H-sets. This procedure is described schematically in the following diagram:

$$\begin{aligned} S_w^R \rightarrow H_{n+1,out} \rightarrow H_{n,in} \rightarrow \cdots \\ \rightarrow H_{i+1,out} \rightarrow H_{i,in} \rightarrow \cdots \\ \rightarrow H_{2,out} \rightarrow H_{1,in} \rightarrow S_w^L. \end{aligned}$$

Note that a jump from one set to the next always happens at the first possible value in the current H-set.

Gimse has shown [24] that the above construction gives a unique solution of the triangular system, if the following conditions hold:

$$(A)\ F_g(0) = 0, \quad (B)\ F_g(1) = 1, \quad (C)\ F_w(S_g, 1 - S_g) = 1 - F_g(S_g)$$

$$(D)\ \frac{\partial F_w}{\partial S_w} \geq 0, \qquad (E)\ \frac{\partial F_w}{\partial S_g} < 0, \qquad (F)\ F_g'(S_g) \geq 0.$$

For a discussion of these conditions we refer to Paper C.

3.3.2 Approximation of a full three-phase flow system by a triangular system

Since the fractional flow function for the gas phase is nearly independent of the water saturation, it seems natural to decouple the gas phase from the other phases. This can be done simply by plugging in a value for the water saturation, S_w^0, in the gas fractional flow function:

$$F_g(S_w, S_g) \approx F_g(S_w^0, S_g) \stackrel{\text{def}}{=} F_g(S_g). \tag{3.12}$$

We can choose S_w^0 so that the decoupled fractional flow function is as close as possible to the complete function in some norm over the admissible section of state space, see [27]. However, in the experiments reported in Paper C, S_w^0 is chosen more or less arbitrary to be zero.

In situations where the full solution for the gas phase consists of two rarefaction waves connected by an intermediate shock wave, the triangular approximation must fail because it cannot produce such a wave structure. A possible solution to this problem is to let S_w^0 be defined locally for each Riemann problem which is solved. This will allow for some feedback, and can be combined with the fact that the total mobility λ_T acts as an approximate invariant for the transport. Thus $\lambda_T(S_w, S_g) \approx \lambda_T(S_w^0, S_g)$ may be used to eliminate S_w from F_g in a more accurate way. However, this idea was not pursued any further in the paper.

Another difficulty that arises from the approximation (3.12), is that condition (C) is violated since

$$F_w(1 - S_g, S_g) = 1 - F_g(1 - S_g, S_g) \neq 1 - F_g(S_w^0, S_g).$$

If condition (C) is not satisfied the construction of the solution may fail in two ways for values close to $S_o = 0$: Either the construction of appropriate H-sets will fail, or the tracking of admissible waves becomes impossible. Since $S_o \approx 0 \implies S_w \approx 1 - S_g$, we may circumvent the problem by replacing S_w^0 with $1 - S_g$ in (3.12) when the oil phase is close to residual. Again, this requires a local definition of S_w^0 which has not been implemented in our simulator yet.

3.4 Concluding remarks

For the detailed discussion of the numerical results, we refer to Paper B and C. A front tracking streamline method (SFTM) for multi-phase flow in porous media was presented. The main advantage of this method is to handle the advective part of the nonlinear transport using streamline information, and still be able to solve for diffusive/dispersive effects on a regular grid. The method has been compared with a Modified Method of Characteristics (MMOC) and a Fast Marching (FMM) approach for two-phase flow problems. The solutions obtained seem to be equally accurate. The SFTM and the MMOC are comparable when it comes to computational efficiency, whereas the FMM gives a much faster advection solver. However, compared to the MMOC and the FMM, the SFTM is more flexible and has less restrictions with respect to the complexity of the problems that may be solved.

Using the H-set method, the SFTM approach has been extended to solve three-phase flow problems which are triangular. Since most three-phase flow problems are fully coupled in both saturations, triangular systems can only be approximate. However, because the viscosity of the gas is much smaller than the viscosities of the liquid phases the gas phase is often nearly decoupled from the other phases. We showed that the solution of a naive triangular approximation of

a fully coupled system, may and may not be a good approximation to the solution of the fully coupled system.

In these two papers standard operator splitting was applied, i.e, without correction in the diffusion step. Including a correction term would possibly give sharper fronts, as explained in Chapter 2. However, defining the residual flux is not straight forward for multi dimensional problems. A main difficulty is to find the correction domain. After obtaining the solution along the streamlines in the hyperbolic step, one needs to project not only the solution, but also the correction interval down onto the grid for the parabolic step. To find a local correction domain, information from several streamlines at a time must probably be used. Hence, it might also be hard to choose the correct shock values.

Chapter 4

Interfacial area and dynamic network models

This chapter covers ideas and results from Paper D, *"Two phase flow including interfacial area as a variable "*, and Paper E, *"A pore network model for calculation of interfacial velocities "*. The work presented is two folded; a generalization of the standard two-phase flow model and testing of this model using a dynamic network model.

Multi-phase porous media systems are characterized by fluid-fluid interfaces that exist at the pore scale. These interfaces define the spatial boundaries of each phase at any given instant in time. Interfaces also have properties such as interfacial tension, which allows each fluid to maintain a different pressure. The resulting difference between individual phase pressures is usually called capillary pressure. Mass is transferred from one fluid phase to another across the fluid-fluid interfaces. Fluid-solid interfaces provide similar surfaces for mass exchanges between fluid and solid phases. For these reasons, an understanding of interfacial behavior at the pore scale, and subsequent scaling of that behavior to the more practical continuum scale, is important to give proper descriptions of porous media flow systems.

4.1 A generalized two phase flow model

As mentioned in the introduction, Section 1.1 on page 3, traditional multi-phase flow models are usually based on direct extensions of one-phase flow equations. These models are ad hoc and involve hidden assumptions that may be difficult to uncover in a practical application. Furthermore, it may not be clear whether all important physical effects are appropriately accounted for in the mathematical formulations. This may also explain the apparent hysteresis in the constitutive

relationships.

A rigorous approach to modeling of multi-phase flow is given by Gray and Hassanizadeh, e.g. [2]. This approach starts from first principles and is aiming at a more complete description of multi-phase flow phenomena. In particular, their theoretical arguments imply that fluid-fluid interfacial areas, a^{wn}, should be primary variables in the mathematical formulation of two-phase flow. Their analysis, based on thermodynamics, also includes other variables, like contact lines and common points, but these will not be considered here. In this theory, it is conjectured that capillary-pressure hysteresis is a consequence of incompleteness of traditional models. A non-hysteretic constitutive relationship would require that the $P_c - s^w$ relationship should be extended by at least a third variable, e.g. P_c, s^w, and a^{wn}. This conjecture has been tested using computational (quasi-static) pore-scale network models, see [28, 29, 30]. The results obtained from these network models give some support to the theoretical conjecture. However, experimental validation is still required.

An important issue is whether the inclusion of interfacial area in a two-phase flow model changes the nature of the solution for the saturation. Of course there are situations where the interface itself is of interest, but in the oil reservoir setting the saturation is what really matters. In Paper D, which is presented in the following sections, this question is addressed and to some degree answered.

4.1.1 Assumptions and governing equations

Following the paper we will take a general set of equations based on the theory of Gray and Hassanizadeh, [2], and reduce them to a system of two equations for saturation and interfacial area using a standard fractional flow formulation. The major assumptions applied are:

1. No phase change occurs;
2. Isothermal system;
3. Immobile, non-deforming solid;
4. Common lines are neglected;
5. The solid-fluid interface dynamics are negligible (i.e no film flow);
6. Massless fluid-fluid interface;
7. Incompressible fluids;
8. Inertial terms are negligible in the momentum equations;
9. Interfacial tensions are all constant and specified.

These assumptions most certainly restrict the applicability of the model, but they are needed to reduce the complexity of the general set of equations. In a preliminary analysis such as this, the model is still useful because it enables us

to get some insight into the properties of two phase flow models that include interfacial area. Notice, that by using this general framework all the assumptions must be clearly stated.

A complete list of equations and variables is found in Paper D. Only the most important equations will be given here. The mass and momentum conservation for each phase is governed by standard equations. The interface was assumed massless and hence there is no mass conservation equation for the interface. The momentum conservation equation for a massless interface indicates that the interfacial velocity is a weighted sum of the velocities of the adjacent phases. Thus, the following equality is assumed:

$$(\mathbf{R}^w_{wn} + \mathbf{R}^n_{wn}) \cdot \mathbf{v}^{wn} = \mathbf{R}^w_{wn} \cdot \mathbf{v}^w + \mathbf{R}^n_{wn} \cdot \mathbf{v}^n \tag{4.1}$$

where $\mathbf{R}^\alpha_{wn}$ is the resistance term for the α-phase due to the wn-interface (fluid-fluid) and $\mathbf{R}^\alpha_{\alpha s}$ the resistance term for the α-phase due to the αs-interface (fluid-solid). $\mathbf{v}^\alpha$ is the velocity of α-phase and $\mathbf{v}^{wn}$ is the velocity of the wn-interface. Resistance terms can be viewed upon as the inverse of conductance and is a function of $\mathbf{K}^{-1}$.

In addition, a geometry equation for interfacial area has to be satisfied:

$$\frac{\partial a^{wn}}{\partial t} + \nabla \cdot [\mathbf{G}^{wn} a^{wn} \cdot \mathbf{v}^{wn}] = 0. \tag{4.2}$$

Here a^{wn} is the specific interfacial area (fluid-fluid) and $\mathbf{G}^{wn}$ is a geometric tensor. Also, the capillary pressure equation

$$\gamma^{wn} J^w_{wn} = p^w - p^n = -P_c \tag{4.3}$$

must hold, where J^w_{wn} is the average curvature and γ^{wn} is the surface tension of the wn-interface.

Equation (4.2) and (4.3) are in fact simplified versions of the corresponding equations arising from the general framework using the assumptions outlined in the start of this section. In Equation (4.2) the production term is neglected. In general, this is a significant assumption that limits the general applicability of the system of equations. However, it will be applied consistently here with the objective of performing a preliminary analysis of a simplified set of equations. Equation (4.3) is reduced from a dynamic capillary equation by neglecting the time derivative of the saturation. We refer to Section 2 in Paper D for the full equations and motivations. Notice, however, that adding a production term in Equation (4.2), might make it hard, if not impossible, to find a fractional flow formulation of the equations.

4.1.2 Fractional flow formulation

By eliminating all variables but saturation and interfacial area, and neglecting the gravity terms, we get the following fractional flow formulation

$$\begin{aligned} \varepsilon \frac{\partial s^w}{\partial t} + \mathbf{u} \cdot \nabla \cdot \mathbf{F}_w &= \nabla \cdot (\mathbf{D}_w \cdot \nabla P_c), \\ \frac{\partial a^{wn}}{\partial t} + \frac{1}{3} \left(\mathbf{u} \cdot \nabla \cdot (\mathbf{F}_{wn} a^{wn}) \right) &= \frac{1}{3} \nabla \cdot (a^{wn} \mathbf{D}_{wn} \cdot \nabla P_c) \end{aligned} \tag{4.4}$$

where $\mathbf{F}_\alpha$ is the fractional flow (of the phase or interface), $\mathbf{D}_\alpha$ is the diffusion function (for the phase or interface), $\mathbf{u}$ is the Darcy velocity and ε is the porosity. This constitutes a 2×2 coupled system for the saturation and the interfacial area.

To close the system we need a constitutive relationship for capillary pressure as a function of saturation and interfacial area. To our knowledge, no such relationship has been determined experimentally. Thus, we construct this relationship based on results from network models, see e.g. [29]. In addition, functional forms of the resistance terms are needed in the fractional flow and diffusion function. Details on this are given in Section 4 of Paper D.

There are two difficulties related to the system in (4.4), and both arise from the capillary pressure relationship. First of all the $P_c - s^w - a^{wn}$ surface is not defined for all value pairs of saturation and interfacial area. This might be solved by some kind of (smooth) extrapolation or extention of the surface. We avoided this problem by doing a careful choice of initial values. This is in general not enough since one cannot guarantee that the solution will stay on the surface. However, it is possible to reformulate the system as a set of equations for saturation and capillary pressure. We did not pursue this in the article, but it is our assumption that this might be less restrictive than the proposed system.

The second problem is that the system in some sense is overdetermined. If the system is solved sequentially, the (new) saturation and the (old) capillary pressure will be available when the interfacial area is solved for. Hence, we are then in the position to get the interfacial area from the capillary pressure relationship without actually solving the equation. This was not investigated any further, but we find it appropriate to point this problem out.

For a numerical example we refer to Paper D again. Some concluding remarks follow in Section 4.3.

4.2 Dynamic network models and equation testing

Network models have been used to investigate physical phenomena in multi phase flow that are hard to observe in laboratory experiments. Typically, these models

have been static in the sense that they just track the interface from one stable position to another without taking time into account. This is sufficient for studying fingering effects, functional relationships that do not depend on time and so on. One example that illustrates what can be achieved by such models, is the determination of a functional relationship between capillary pressure, saturation and interfacial area, see e.g. [29].

The view that interfacial area plays an important role in porous media flows is supported by the already mentioned theoretical developments reported by Gray and Hassanizadeh, [2]. In their work, a thermodynamic approach is used to show that the relationship between capillary pressure and saturation is incomplete, and that interfacial area should enter into the relationship.

One of the problems associated with tests of theories involving interfacial area, is the lack of experimental validation. It is very difficult to determine interfacial area, and even more difficult to determine interfacial dynamics, which tends to occur on very short time scales. Therefore, testing of these theories must rely on using specific kinds of computational models, including so-called pore-scale network models. Pore-scale network models typically represent the pore space of the medium using simplified geometries. Within this geometric representation equations are solved to explicitly track the location of all fluid-fluid interfaces within the network.

The models are often run to mimic typical laboratory experiments, such as pressure cell tests to determine the relationship between capillary pressure and relative fluid saturation. This is accomplished by using lattices that are sufficiently large to define meaningful continuum-scale measures, such as fluid saturation. In other words, the network should represent one or more REVs. Results of such simulations show all of the major features of experimental relationships, including finite entry pressures, residual saturations, and hysteresis.

Two general types of pore-scale network models may be identified: quasi-static models and dynamic models. In a quasi-static model, the location of any fluid-fluid interface is governed by equilibrium considerations only. Equilibrium states are determined from the Young-Laplace equation, which relates the capillary pressure to the interfacial tension and the interface curvature, viz.

$$P_c = \frac{\sigma}{R}. \tag{4.5}$$

In this equation, σ is the interfacial tension and R is the radius of curvature. For a given imposed capillary pressure there are rules to determine whether or not an interface is stable at a given location. If the interface is unstable, it is moved through the network until a stable position is found, or until it exits the network. No time dependence is included in the calculation. Examples of these kinds of models include those described by Dullien [31], Ferrand and Celia [32], and Reeves [28].

A second type of pore network model involves computation of transient behavior associated with interface movement. That is, unstable interfaces are tracked through the network until a stable position is reached, but the transient nature of the movement from one position to another is explicitly described and modeled. Most pore-scale network models reported in the literature are quasi-static, but there are several dynamic models that have been developed. These include the model of Blunt and King [33]; a series of models by Payatakes and coworkers (see, for example, Valavanides and Payatakes [34]), and more recent models by Mogensen and Stenby [35], Aker et al. [36], Hassanizadeh (Dijkstra et al. [37]) and by Dahle and Celia [38]. The models of Payatakes are the most comprehensive, including a focus on mobilization of trapped fluids and so-called drop traffic flows.

To study the equations in the generalized two phase flow model in Section 4.1, static network models are not sufficient; we need dynamic network models. In Paper E, we used a model based on the original work of Blunt and King [33] and calculated dynamic interfacial behavior, with focus on volume-averaged interfacial velocity. The most important features of the model are described, and a definition of average interfacial velocity is provided, in the next section. In the paper specific calculations were performed to demonstrate how continuum-scale measures of both interface velocity and phase velocity can be quantified. The model was then used to test a specific theoretical conjecture regarding interfacial velocity and its relationship to average phase velocities.

4.2.1 The dynamic network model

The pore-scale network model used in Paper E is an extension of the model of Blunt and King [33]. The pore network is a rectangular lattice, with spherical pore bodies and cylindrical pore throats, with pore-size distributions defined for the bodies and throats, see Figure 4.1 below. Following Blunt and King [33], the model is simplified by the following assumptions:

1. Local capillary pressure in the pore throats is assumed to be negligible, so that only one pressure exists within a pore body, independent of the local saturation of that pore body.
2. While the radius of a pore throat serves to define its hydraulic conductance, the volume contributed by the pore throat is assumed to be small relative to volumes of pore bodies. Therefore, movement of an interface through a pore throat is assumed to occur instantaneously.
3. Flow within pore throats is assumed to be laminar and given by Poiseuille's law, see Equation (4.8) and (4.7).
4. Both fluids are assumed to be incompressible.

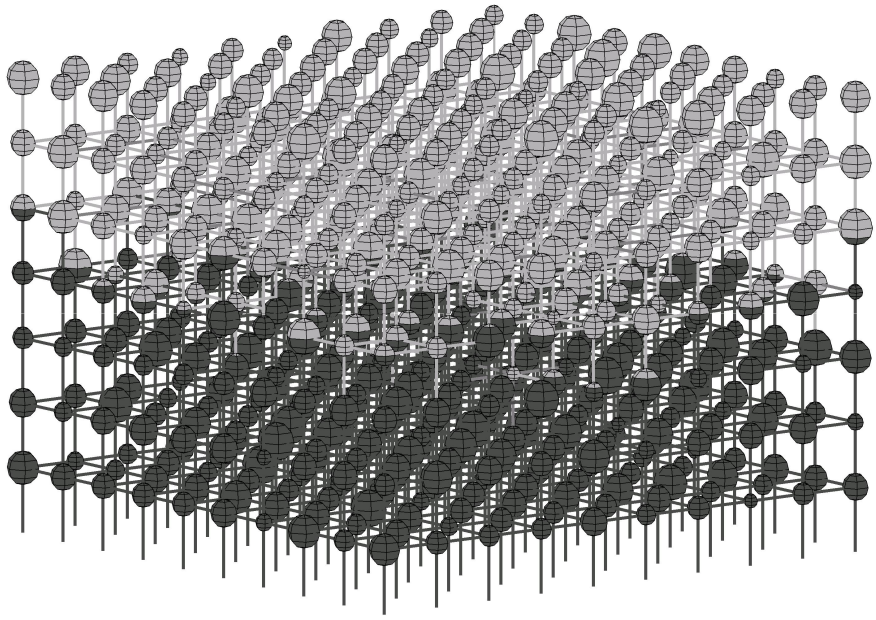

Figure 4.1: Example of a network model showing stable displacement.

With these assumptions, the set of governing equations is relatively simple. Each equation must obey volume conservation within each pore body, such that

$$V_i \frac{\partial S_i^\alpha}{\partial t} + \sum_{j \in N_i} Q_{ij}^\alpha = 0. \tag{4.6}$$

Here V_i represents the volume of pore body i, S^α represents local saturation (percent of V_i filled with fluid α), Q_{ij}^α is the volumetric flux from pore body i to it's neighbor j, and N_i is a list of all neighbor pore bodies for pore body i. This equation is written for both fluid phases, wetting ($\alpha = w$) and non-wetting ($\alpha = n$). The volumetric flux is related to pressures at the pore bodies by Poiseuille's law,

$$Q_{ij}^\alpha = G_{ij}^\alpha (p_i^\alpha - p_j^\alpha) \tag{4.7}$$

where p_l^α represents pressures, and G_{ij}^α represents hydraulic conductance in the pore throat connecting pore bodies i and j. Because the pore throats are cylindrical and interface movement through them is instantaneous, only one fluid can occupy a given pore throat at a given time. Therefore, the fluid occupying the pore throat has conductance

$$G_{ij}^\alpha = \frac{\pi r_{ij}^4}{8 \mu^\alpha l_{ij}}, \tag{4.8}$$

while the non-occupying fluid has zero conductance. Here r_{ij} and l_{ij} is the radius and the length of the pore throat, respectively. Summation of Equation (4.6) over the two phases gives the equation

$$\sum_{j \in N_i} (Q_{ij}^w + Q_{ij}^n) = 0 \tag{4.9}$$

Substitution of Equation (4.7) for each of the phase fluxes Q_{ij}^α provides a set of algebraic equations with the pore-body pressures as unknowns. These can be solved using standard matrix solution methods. Time steps are chosen so that during any time step, only one pore body reaches full non-wetting phase saturation.

As the model size increases the matrix solver becomes very important. The matrix is sparse, banded and also symmetric if contributions from boundary (and trapped) pore bodies are moved to the right hand side. However, having a condition number of 10^{-8} or more, the matrix system is hard to solve. Using a direct solver will slow the computations down dramatically even for matrices with narrow band width. We used a preconditioned conjugate gradient method with incomplete Cholesky factorization as preconditioner, and it worked very well. For a network with 5000 nodes the speed-up compared to a direct solver was only four, but for a network with 50000 nodes the speed-up was over 100. These results are for illustration only since we did not do a rigorous convergence test. The number of off diagonal rows that are non-zero is equal to the maximal coordination number of the nodes. For a three dimensional rectangular lattice the maximal coordination number is six, i.e, one node can be connected to six other nodes. For a irregular lattice this number may increase and having a good matrix solver is even more important.

Overall, the algorithm proceeds as an Implicit Pressure Explicit Saturation (IMPES) routine. The major unknowns are the pressure and saturation of each pore body. For a given distribution of fluids, phase conductances are calculated and substituted into Equation (4.9), which is solved for a new pressure field. That pressure field is then used in Equation (4.7) to compute fluxes through the pore throats. These fluxes are then used (in conjunction with knowledge of the current saturations in each pore body) to determine the minimum filling time for each of the pores, and this is set as the time step size. Then Equation (4.6) is used to update the saturations in each pore body. Newly created interfaces are tested for stability, conductances are updated, and the procedure is repeated.

4.2.2 Calculating average variables

Following the article we now define average variables over a representative volume. The volume might be chosen to correspond to the entire volume of the

network, or it might be defined as essentially two-dimensional slices through the network in the direction perpendicular to the macroscopic direction of displacement. In either case, the volume-averaged saturation is defined as

$$S^{\alpha} = \frac{\sum_{i \in N_{vol}} V_i S_i^{\alpha}}{\sum_{i \in N_{vol}} V_i} = \frac{1}{V} \sum_{i \in N_{vol}} V_i S_i^{\alpha} \tag{4.10}$$

where V is the volume of the chosen averaging region, and N_{vol} denotes the set of pore bodies within the chosen averaging volume. Capillary pressure is defined as the difference between volume-averaged phase pressures, such that

$$P_c = p_n - p_w = \frac{1}{V}\Big(\sum_{i \in N_{vol}} V_i S_i^n p_i - \sum_{i \in N_{vol}} V_i S_i^w p_i \Big). \tag{4.11}$$

Here p_i corresponds to the pressure in pore body i. Notice that while no local capillary pressure exists (by assumption in the model), a macroscopic capillary pressure is still well defined based on the average phase pressures.

Average properties associated with interfaces require somewhat more care in their definitions. Because no capillary pressure is associated with individual pore bodies, the shape (especially the curvature) of a particular interface is not specified. The only information for active (non-trapped) interfaces is that they reside in a specific pore body. The interfacial area in a pore body is of course a function of saturation, but for simplicity we assumed it to be constant equal to the cross section of the pore body. Those interfaces trapped at the entrance of pore throats are assigned the area associated with the diameter of the pore throat. Therefore, the specific interfacial area (defined as the amount of interfacial area per unit volume of porous medium) is defined as

$$a^{wn} = \frac{1}{V}\Big(\sum_{i \in N_{vol}} a_i^{wn} + \sum_{j \in M_{vol}} a_j^{wn} \Big) = \frac{A^{wn}}{V} \tag{4.12}$$

where M_{vol} denotes the set of pore throats that are contained within the averaging volume V.

The averaged variable that is the most difficult to define is the volume-averaged interfacial velocity. To define a finite local velocity that preserves proper global velocities, the pore filling associated with saturation changes is extended in length to cover the combined pore body – pore throat combination. The 'locally averaged' velocity for a specific interface is defined as

$$\|\mathbf{v}_i^{wn}\| = l_{i,j} \frac{\Delta S_i^n}{\Delta t}. \tag{4.13}$$

The double brackets signify magnitude of the interface velocity vector, the length $l_{i,j}$ denotes the length of the pore throat through which the entering interface travels plus the diameter of the pore body i, and ΔS_i^n denotes the saturation change over the time interval Δt. The direction assigned to the interfacial velocity vector is the average of the total inflow vector and total outflow vector. Finally, the volume-averaged velocity vector is given by the sum of each interfacial velocity weighted by the area of the interface,

$$\mathbf{v}^{wn} = \frac{1}{A^{wn}} \sum_{i \in N_{vol}} \mathbf{v}_i^{wn} a_i^{wn} \tag{4.14}$$

Volume-averaged phase velocities may be defined analogously to average interfacial velocities with volume replacing areas as the appropriate weights. Hence,

$$\mathbf{v}^{\alpha} = \frac{1}{V S^{\alpha}} \sum_{i \in N_{vol}} \mathbf{v}_i^{\alpha} V_i S_i^{\alpha} \tag{4.15}$$

where $\mathbf{v}_i^{\alpha}$ is given by an equation similar to Equation (4.13), with appropriate modification for the case of $S = 1$ or $S = 0$.

Another possible definition of velocities arises if we consider the flow in the pore throats and pore bodies separately. Let

$$\|\mathbf{v}_{jt}^{\alpha}\| = \frac{r_j^2}{8\mu^{\alpha} l_j} \|\Delta p_j\| \tag{4.16}$$

and

$$\|\mathbf{v}_{ib}^{\alpha}\| = 2R_i^2 \frac{\Delta S_i^n}{\Delta t} \tag{4.17}$$

be the phase velocity in pore throat j and pore body i, respectively. For the throats the actual flux is used to find the velocity, and for the pore bodies a 'locally averaged' velocity. Then we define the volume-averaged phase velocity as

$$\mathbf{v}^{\alpha} = \frac{1}{V S^{\alpha}} \Big(\sum_{i \in N_{vol}} \mathbf{v}_{ib}^{\alpha} V_{ib} S_i^{\alpha} + \sum_{j \in M_{vol}} \mathbf{v}_{jt}^{\alpha} V_{jt} \Big), \tag{4.18}$$

and the volume-averaged interface velocity analogously. This definition was not used in the article since it did not reveal any new information, i.e, the results from the equation testing were qualitatively the same.

4.2.3 Equation testing

In Paper E we wanted to test Equation (4.1). The following procedure was used: The phase velocities from the network model were used to get the theoretical interface velocity which then was compared to the interface velocity from the network

model. As the numerical results from the paper show, the match depends on the flow regime, i.e., stable or unstable, and whether or not the trapped interfaces are included.

In Paper D we did not discuss the freedom associated with Equation (4.1). For a scalar **K** we get the following expression for the interface velocity

$$\mathbf{v}^{wn} = F^w\mathbf{v}^w + F^n\mathbf{v}^n = \frac{f^w}{f^w + f^n}\mathbf{v}^w + \frac{f^n}{f^w + f^n}\mathbf{v}^n \tag{4.19}$$

where

$$f^w = \mu^w h^w(s^w)(s^w)^2,$$
$$f^n = \mu^n h^n(s^n)(s^n)^2,$$

when the definitions of the resistance terms from Paper D are used. For h^α we assume a more general form than was used in the article, namely

$$h^\alpha(s^\alpha) = \beta^\alpha(1 - s^\alpha)^p \tag{4.20}$$

To determine the β-parameters we put the following restrictions on F^α:

$$\lim_{s^w \to 1} F^w(s^w) = 0 \tag{4.21}$$
$$\lim_{s^w \to 0} F^w(s^w) = 1 \tag{4.22}$$
$$\lim_{s^w \to 1} F^n(s^n) = \lim_{s^n \to 0} F^n(s^n) = 1 \tag{4.23}$$
$$\lim_{s^w \to 0} F^n(s^n) = \lim_{s^n \to 1} F^n(s^n) = 0 \tag{4.24}$$

These restrictions are motivated by the observation that the interface velocity is close to the non-wetting phase velocity when the drainage starts and close to the wetting phase velocity when close to residual saturation. Below, the limits are displayed for different choices of p:

	$p = 1$	$p = 2$	$p > 2$
$\lim_{s^w \to 1} F^w(s^w)$	1	L^w	0
$\lim_{s^w \to 0} F^w(s^w)$	0	L^w	1
$\lim_{s^w \to 1} F^n(s^n)$	0	L^n	1
$\lim_{s^w \to 0} F^n(s^n)$	1	L^n	0

The entity L^α is given by $L^\alpha = \mu^\alpha\beta^\alpha/(\mu^w\beta^w + \mu^n\beta^n)$. We observe that p has to be larger than two in order to satisfy Equation (4.21) - (4.24). We do not get any constraints on the choice of β^α. Actually, several test cases showed that the best

choice (measured in the quality of the match between the theoretical and network model interface velocity) was $\beta^\alpha = 1/\mu^\alpha$. Together with the choice of p equal to three, this defined the relationship between the volume-averaged interface velocity and the volume-averaged phase velocities that we tested in the article.

4.3 Concluding remarks

In Paper D initial numerical solutions for an enhanced model of two phase flow which includes fluid-fluid interfacial area as a primary variable were presented. For the particular case studied, the saturation profiles show little dependency on interfacial area. Since the correct functional forms of the resistance terms used in the model are not known, more general studies are required to assess the practical importance of the interfacial area equations to flow modeling. In addition, numerical solutions need to be obtained for cases where the simplifying assumptions applied to the governing equations are systematically examined. The results in this paper represent a starting point for this more general analysis.

While we cannot reach any general conclusions based on our initial calculations, we can make a few general observations. First, inclusion of the interfacial area equations allows for direct calculation of the amount of interfacial area in the system. Equations written for the individual phases also incorporate effects of the interfaces through functional dependencies in the appropriate nonlinear coefficients. In addition, inclusion of a unique functional relationship between P_c, s^w, and a^{wn}, allows hysteresis within the $P_c - s^w$ plane to be incorporated into the algorithm with no additional effort. Arbitrary drainage and imbibition cycles can be simulated without redefining the constitutive curves. This appears to be a major advantage of this approach to multi phase flow modeling. The cost of such additional generality and flexibility is the need to identify and quantify additional parameters, as well as their functional dependencies on interfacial area. Additional equations also need to be solved compared to the traditional equations for multi phase flow.

The overall significance of interfacial areas in the mathematical description of multi phase flow in porous media, remains to be determined. The degree to which the governing equations can be simplified, must be explored numerically. This requires a systematic and comprehensive numerical approach. The results presented in Paper D represent a first contribution to the overall numerical study.

The dynamic network model presented in Paper E is relatively simple and leads to numerical calculations that are straight-forward to implement. The calculation of averages allows many continuum-scale variables to be calculated, and thereby facilitates testing of new theories that involve non-traditional variables. We focused on interfacial dynamics, and calculation of average interfacial ve-

locities. The results were used to test a specific conjecture that relates average interfacial velocity to average phase velocities.

In particular, we conclude that the proposed equation that relates interfacial velocity to phase velocities only hold under very specific conditions, namely piston-like stable displacements in which trapped interfaces are neglected. Under more general conditions the equation provides a poor prediction. To close the extended set of equations for two-phase flow, which include specific interfacial area as a primary variable, new constitutive equations need to be developed.

While Paper E focused on a specific constitutive equation, the general approach is illustrative for the kind of problems that can be solved with dynamic pore-scale network models. Because the local-scale information is highly detailed, many upscaled variables can be calculated. This greatly facilitates testing of new theories, and has the potential to provide significantly improved insight into fundamental behavior of two-phase porous media flows.

Chapter 5

Conclusions

This chapter contains a summary of conclusions and remarks made in the previous chapters. Since the presented work is done in collaboration with other researchers, I will also point out some of my main contributions.

Corrected operator splitting for systems. In Paper A results for two particular 2×2 systems describing flow in porous media were presented. Simulations for a two-phase multicomponent model, a polymer system, and for a triangular three-phase flow model were reported. In addition, the polymer system was solved in 2D using dimensional splitting.

We demonstrate numerically that operator splitting (OS) methods for systems of convection-diffusion equations in one space dimension, have a tendency to be too diffusive near viscous shock waves. The idea behind the scalar COS method is to use the wave structure from the convection step to identify where the nonlinear splitting error (or entropy loss) occurs. The potential error is then compensated for in the diffusion step (or in a separate correction step).

Similar to the scalar case, the splitting error is closely related to the local linearizations introduced implicitly in the convection steps due to the use of an entropy condition. A COS method for systems was proposed. The numerical examples demonstrate that the COS method is significantly more accurate than the corresponding OS method when the splitting step is large and the solution consists of (moving) viscous shock waves.

My contributions: The triangular three-phase flow solver was implemented by me, using the theory in [24]. To our knowledge this was the first attempt to solve this system using a COS method. In the process I also contributed to the general methodology and to the definition of the residual flux for systems.

Front tracking along streamlines. For the detailed discussion of the numerical results, we refer to Paper B and C. A front tracking streamline method (SFTM) for multi-phase flow in porous media was presented. The main advantage of this method is to handle the advective part of the nonlinear transport using streamline information, and still be able to solve for diffusive/dispersive effects on a regular grid. The method has been compared with a Modified Method of Characteristics (MMOC) and a Fast Marching (FMM) approach for two-phase flow problems. The solutions obtained seem to be equally accurate. The SFTM and the MMOC are comparable when it comes to computational efficiency, whereas the FMM gives a much faster advection solver. However, compared to the MMOC and the FMM, the SFTM is more flexible and has less restrictions with respect to the complexity of the problems that may be solved.

Using the H-set method, the SFTM approach has been extended to solve three-phase flow problems which are triangular. Since most three-phase flow problems are fully coupled in both saturations, triangular systems can only be approximate. However, because the viscosity of the gas is much smaller than the viscosities of the liquid phases the gas-phase is often nearly decoupled from the other phases. We showed that the solution of a naive triangular approximation of a fully coupled system, may and may not be a good approximation to the solution of the fully coupled system.

In these two papers standard operator splitting was applied, i.e, without correction in the diffusion step. Including a correction term would possibly give sharper fronts, as explained in Chapter 2. However, defining the residual flux is not straight forward for multi dimensional problems. A main difficulty is to find the correction domain. After obtaining the solution along the streamlines in the hyperbolic step, one needs to project not only the solution, but also the correction interval down onto the grid for the parabolic step. To find a local correction domain, information from several streamlines at a time must probably be used. Hence, it might also be hard to choose the correct shock values.

My contributions: I implemented the three phase streamline solver, most of the two phase streamline solver and the streamline generator (for a given velocity field). I would like to thank Knut A. Lie for letting me use his front tracker code and Johnny Frøyen for the pressure/velocity solver. I contributed strongly to the development of these methods and in particular with questions related to triangular systems.

Interfacial area and dynamic network models. In Paper D initial numerical solutions for an enhanced model of two phase flow which includes fluid-

fluid interfacial area as a primary variable were presented. For the particular case studied, the saturation profiles show little dependency on interfacial area. Since the correct functional forms of the resistance terms used in the model are not known, more general studies are required to assess the practical importance of the interfacial area equations to flow modeling. In addition, numerical solutions need to be obtained for cases where the simplifying assumptions applied to the governing equations are systematically examined. The results in this paper represent a starting point for this more general analysis.

While we cannot reach any general conclusions based on our initial calculations, we can make a few general observations. Firstly, inclusion of the interfacial area equations allows for direct calculation of the amount of interfacial area in the system. Equations written for the individual phases also incorporate effects of the interfaces through functional dependencies in the appropriate nonlinear coefficients. In addition, inclusion of a unique functional relationship between P_c, s^w, and a^{wn}, allows hysteresis within the $P_c - s^w$ plane to be incorporated into the algorithm with no additional effort. Arbitrary drainage and imbibition cycles can be simulated without redefining the constitutive curves. This appears to be a major advantage of this approach to multi phase flow modeling. The cost of such additional generality and flexibility is the need to identify and quantify additional parameters, as well as their functional dependencies on interfacial area. Additional equations also need to be solved compared to the traditional equations for multi phase flow.

The overall significance of interfacial areas in the mathematical description of multi phase flow in porous media, remains to be determined. The degree to which the governing equations can be simplified, must be explored numerically. This requires a systematic and comprehensive numerical approach. The results presented in Paper D represent a first contribution to the overall numerical study.

The dynamic network model presented in Paper E is relatively simple and leads to numerical calculations that are straight-forward to implement. The calculation of averages allows many continuum-scale variables to be calculated, and thereby facilitates testing of new theories that involve non-traditional variables. We focused on interfacial dynamics, and calculation of average interfacial velocities. The results were used to test a specific conjecture that relates average interfacial velocity to average phase velocities.

In particular, we conclude that the proposed equation that relates interfacial velocity to phase velocities only hold under very specific conditions, namely

piston-like stable displacements in which trapped interfaces are neglected. Under more general conditions the equation provides a poor prediction. To close the extended set of equations for two-phase flow, which include specific interfacial area as a primary variable, new constitutive equations need to be developed.

While Paper E focused on a specific constitutive equation, the general approach is illustrative for the kind of problems that can be solved with dynamic pore-scale network models. Because the local-scale information is highly detailed, many upscaled variables can be calculated. This greatly facilitates testing of new theories, and has the potential to provide significantly improved insight into fundamental behavior of two-phase porous media flows.

My contributions: In Paper D the major part of the development of the general two phase flow model and the implementation of the numerical solver was done by me. In Paper E an existing network model was improved and extended by me to allow for calculation of several average variables and general rectangular geometry. In addition I was a major contributor in the discussions concerning the definition of average quantities based on the pore scale calculations.

Bibliography

[1] K. Aziz and A. Settari, *Petroleum Reservoir Simulation*. Elsevier Applied Science Publishers, 1985.

[2] W. Gray and S. Hassanizadeh, "Macroscale continuum mechanics for multiphase porous-media flow including phases, interfaces, common lines and common points," *Advances in Water Resources*, vol. 21, no. 4, pp. 261–281, 1998.

[3] G. Dagan, *Flow and transport in porous formations*. Springer-Verlag, 1989.

[4] K. Morton, *Numerical Solution of Convection-Diffusion Problems*. Chapman & Hall, 1996.

[5] M. Espedal and K. Karlsen, "Numerical solution of reservoir flow models based on large time step operator splitting algorithms," in *Filtration in porous media and industrial application (Cetraro, 1998)*, pp. 9–77, Berlin: Springer, 2000.

[6] H. Dahle, *Adaptive characteristic operator splitting techniques for convection-dominated diffusion problems in one and two space dimensions*. PhD thesis, Dept. of Mathematics, Univ. of Bergen, Norway, 1988.

[7] K. Karlsen, K. Brusdal, H. Dahle, S. Evje, and K.-A. Lie, "The corrected operator splitting approach applied to a nonlinear advection-diffusion problem," *Comput. Methods Appl. Mech. Engrg.*, vol. 167, no. 3-4, pp. 239–260, 1998.

[8] K. Karlsen and N. Risebro, "An operator splitting method for nonlinear convection-diffusion equations," *Numer. Math.*, vol. 77, no. 3, pp. 365–382, 1997.

[9] M. Espedal and R. Ewing, "Characteristic Petrov-Galerkin subdomain methods for two-phase immiscible flow," *Comput. Methods Appl. Mech. Engrg.*, vol. 64, no. 1-3, pp. 113–135, 1987.

[10] K. Karlsen and N. Risebro, "Corrected operator splitting for nonlinear parabolic equations," *SIAM J. Num. Anal.*, vol. 37, no. 3, pp. 980–1003 (electronic), 2000.

[11] O. Oleinik, "Discontinuous solutions of non-linear differential equations.," *Amer. Math. Soc. Transl. Ser. 2*, vol. 26, pp. 95–172, 1963.

[12] N. Risebro, "A front-tracking alternative to the random choice method," *Proc. Amer. Math. Soc.*, vol. 117, no. 4, pp. 1125–1139, 1993.

[13] N. Risebro and A. Tveito, "Front tracking applied to a non-strictly hyperbolic system of conservation laws," *SIAM J. Sci. Statist. Comput.*, vol. 12, no. 6, pp. 1401–1419, 1991.

[14] N. Risebro and A. Tveito, "A front tracking method for conservation laws in one dimension," *J. Comput. Phys.*, vol. 101, no. 1, pp. 130–139, 1992.

[15] J. Strikwerda, *Finite difference schemes and partial differential equations*. Pacific Grove, CA: Wadsworth & Brooks/Cole Advanced Books & Software, 1989.

[16] D. Hoff and J. Smoller, "Error bounds for finite-difference approximations for a class of nonlinear parabolic systems," *Math. Comp.*, vol. 45, no. 171, pp. 35–49, 1985.

[17] A. Datta-Gupta and M. King, "A semianalytic approach to tracer flow modeling in heterogeneous permeable media," *Adv. in Wat. Res.*, vol. 18, pp. 9–24, 1995.

[18] T. A. Hewett and T. Yamada, "Theory for the semi-analytical calculation of oil recovery and effective relative permeabilities using streamtubes," *Adv. in Wat. Res.*, vol. 20, pp. 279–292, 1997.

[19] M. King and A. Datta-Gupta, "Streamline simulation: A current perspective," *In Situ (Special Issue on Reservoir Simulation)*, vol. 22, no. 1, pp. 99–139, 1998.

[20] G. Chavent and J. Jaffre, *Mathematical models and finite elements for reservoir simulation*, vol. 17 of *Studies in mathematics and it's applications*. North Holland, Amsterdam, 1986.

[21] Z. Chen and R. Ewing, "Comparison of various formulations of three-phase flow in porous media," *Journal of Computational Physics*, vol. 132, pp. 362–373, 1997.

[22] H. Dahle, M. Espedal, and O. Sævareid, "Characteristic, local grid refinement techniques for reservoir flow problems," *Int. J. for Numerical Methods in Enginering*, vol. 34, no. 3, pp. 1051–1069, 1992.

[23] H. Holden, L. Holden, and R. Høegh-Krohn, "A numerical method for first order nonlinear scalar conservation laws in one dimension.," *Comp. Math. Appl.*, vol. 15, pp. 595–602, 1988.

[24] T. Gimse, "A triangular riemann solver.," Master's thesis, Dept. of Mathematics, Univ. of Oslo, Norway, 1988.

[25] T. Gimse, "A numerical method for a system of equations modelling one-dimensional three-phase flow in a porous medium," in *Nonlinear hyperbolic equations—theory, computation methods, and applications (Aachen, 1988)*, pp. 159–168, Braunschweig: Vieweg, 1989.

[26] L. Holden and R. Høegh-Krohn, "A class of n nonlinear hyperbolic conservation laws.," *Journal of Differential Equations*, vol. 84, pp. 73–99, 1990.

[27] H. Nordhaug, "On solving a three phase flow model with capillary forces," Master's thesis, Dept. of Mathematics, Univ. of Bergen, Norway, 1998.

[28] P. Reeves, *The Development of Pore-scale Network Models for the Simulation of Capillary Pressure - Saturation - Interfacial Area - Relative Permeability Relationships in Multi-fluid Porous Media*. PhD thesis, Department of Civil Engineering and Operations Research, Princeton University, 1997.

[29] P. Reeves and M. Celia, "A functional relationship between capillary pressure, saturation, and interfacial area as revealed by a pore-scale network model," *Water Resources Research*, vol. 32, no. 8, pp. 2345–2358, 1996.

[30] R. Held and M. Celia, "Modeling support of functional relationships between capillary pressure, saturation, interfacial area, and common lines," *Advances in Water Resources*, vol. 24, no. 3-4, pp. 325–343, 2001.

[31] F. Dullien, *Porous Media: Fluid Transport and Pore Structure*. Academic Press, 2 ed., 1992.

[32] L. Ferrand and M. Celia, "The effect of heterogeneity on the drainage capillary pressure - saturation relation," *Water Resources Research*, vol. 28, no. 3, pp. 859–870, 1992.

[33] M. Blunt and P. King, "Relative permeabilities from 2-dimensional and 3-dimensional pore-scale network modeling," *Transport in porous media*, vol. 6, no. 4, pp. 407–433, 1991.

[34] M. Valavanides and A. Payatakes, "True-to-mechanism model of steady-state two-phase flow in porous media, using decomposition into prototype flows," *Advances in Water Resources*, vol. 24, no. 3-4, pp. 385–407, 2001.

[35] K. Mogensen and E. Stenby, "A dynamic two-phase pore-scale model for imbibition," *Transport in Porous Media*, vol. 32, pp. 299–327, 1998.

[36] E. Aker, K. Maloy, A. Hansen, and G. Batrouni, "A two-dimensional network simulator for two-phase flow in porous media," *Transport in Porous Media*, vol. 32, pp. 163–186, 1998.

[37] T. Dijkstra, G. Bartelds, J. Bruining, and S. Hassanizadeh, "Dynamic pore-scale network for two-phase flow," in *Characterization and Measurement of the Hydraulic Properties of Unsaturated Soils* (van Genuchten et al., ed.), pp. 63–69, 1999.

[38] H. Dahle and M. Celia, "A dynamic network model for two-phase immiscible flow," *Computational Geosciences*, vol. 3, pp. 1–22, 1999.

Part II

Published and submitted work